

**AGATA**

**Advance GAMMA Tracking Array**



A project work by

**SHANTONU BISWAS**

[shantobis@gmail.com](mailto:shantobis@gmail.com)

[fys11sbi@student.lu.se](mailto:fys11sbi@student.lu.se)

Supervising of

**JOAKIM CEDERKÄLL**

[Joakim.Cederkall@nuclear.lu.se](mailto:Joakim.Cederkall@nuclear.lu.se)

[joakim.cederkall@cern.ch](mailto:joakim.cederkall@cern.ch)



## Introduction:

Understanding nuclear structure remains a main question to physicists today. Still the structure of nuclei with more than few nucleons is not fully understood. Measuring nuclear excitations might be a tool to solve this puzzle because with extreme conditions the nucleus produce high  $\gamma$ -ray that can be used to compare with model. So, studying the  $\gamma$ -ray with high accuracy is a major key to study the nucleus as well as the universe.

AGATA is a project to track gamma ray with high efficiency, it is a European collaboration project funded by twelve countries in Europe. The project was proposed in 2001 and in 2002 it was signed by the participant countries; in 2005 the first detector showed its result. It is expected that the complete AGATA array will be ready within 2018. The spectrometer is  $4\pi$   $\gamma$ -ray detector which is a combination of several Germanium detectors. It is a major instrument to study nuclear structure ray tracking by measuring the  $\gamma$ -radiation. AGATA will have very good *full energy peak efficiency* with *high peak-to-total ratio* (P/T) and *angular resolution*. The system will be capable of *high event rates* with *ancillary detectors* to measure light charged particles or neutron. In this paper, a short discussion about the project and the physics behind it is presented. A comparison of this  $\gamma$ -tracking array with other  $\gamma$ -tracking arrays has been given with some examples.

## AGATA Physics case:

A major advancement of detector technology for nuclear physics is the development of a gamma-ray detection system which is capable of tracking the location of the energy deposited at every gamma-ray interaction point in a detector. It will provide an unparalleled level of detection sensitivity which will open new avenues for nuclear structure studies.

### **Robustness of the shell structure away from stability:**

A many fermion system like atomic nucleus is described in the approximation of almost independent particles that move in a common potential. This approximation results in a single-particle shell structure of nucleus.

By measuring the electric quadrupole B (E2) strength decoupling or strong polarization effects in nuclei can be searched for. This is sensitive to the proton contribution of the excitation along a single magic isotopic chain. As an example, Coulomb excitation experiments give access to the energy of the first  $2^+$  state and the associated B (E2) transition rate in even-even nuclei. Changes of shell gaps and shifts of the magic gaps can be localized when data are analyzed symmetrically as a function of the proton and neutron numbers. The orbit dependent interaction between neutrons and protons cause this change. AGATA will allow performing these experiments further from stability cause of its increased number of segments.

The low lying vibrational states near closed-shell nuclei is one of the excited modes of interest. It has been shown by comparison with the shell model that a larger effective charge is needed to reproduce the experimental B (E2) values compared to higher mass isotopes which indicate a greater core polarization due to particle-hole excitations. The additional important information on the physics of neutron-rich nuclei can be obtained by higher spin states. If the neutron skin rotates but the core makes no contribution then the observation of excited states will provide information about the neutron-neutron correlations within the surface region. An important way to understand collective excitations

in atomic nuclei is through measurements of electromagnetic moments. Several techniques have been developed and used in different laboratories for this measurement. The sensitivity and the detection efficiency for this important class of experiments have been increased by the AGATA detectors.

### Isospin degrees of freedom: N=Z nuclei:

The unique characteristics for the nuclei  $N = Z$  is: the neutrons and the protons occupy the same orbitals and have maximum spatial overlap of their wave functions, and the charge-independence of the nuclear force gives rise to neutron-proton symmetry which manifests itself in some structure features observable only on the  $N = Z$  or very near to it.

Observation of isospin forbidden E1 gamma transitions in the even-even  $N = Z$  nuclei and differences in E1 transition in mirror nuclei may be used to determine the origins of the isospin symmetry breaking. Heavier  $N = Z$  nuclei are very difficult to study because in fusion-evaporation reactions with stable targets/beams, they are produced with very low cross section and the existing results have exhausted the gamma detection. In such cases the use of a gamma ray detector array with high granularity and efficiency is essential. The performance of AGATA is satisfactory with this experiment.

## Gamma-ray Interactions:

To track the  $\gamma$  ray we must know the individual interactions of an event that can occur inside the detector using the energy and the position of the interaction to reconstruct the sequence of their scattering. When a  $\gamma$ -ray passes through matter, there are mainly three types of interactions: Photoelectric effect, Compton scattering and Pair production.

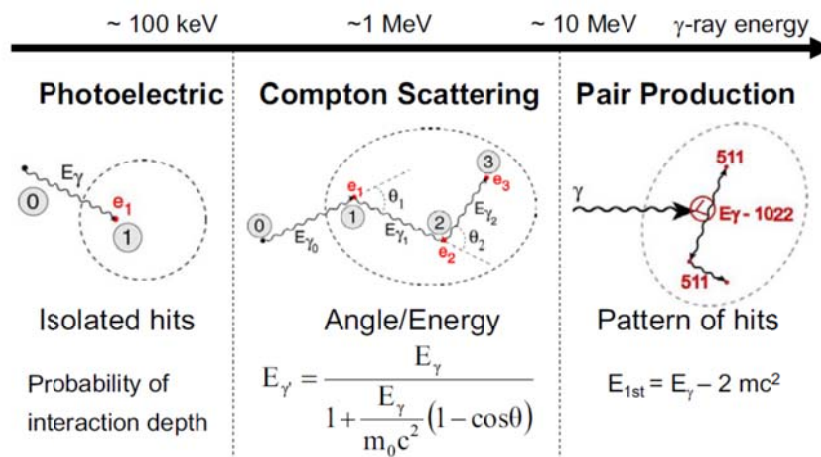


Fig-1: The three probabilities that can occur when photon interacts with matter [7].

### Photoelectric effect:

Low energy gamma rays with the energy range  $\sim 100$  keV interact with an atomic electron and transfer their energy to the electron to eject it from the atom. This absorption of  $\gamma$ -ray occurs in a single point. It is difficult to decide for sure whether low energy absorption is photoelectric absorption or Compton scattering. To determine these points inside the crystal we have to rely on the probability of the  $\gamma$ -ray to reach the interaction positions.

The kinetic energy of the ejected photoelectron is equal to the difference of the incident  $\gamma$ -ray and the binding energy of the electron. Below 50 keV the photoelectric effect is the dominating energy transfer mechanism.

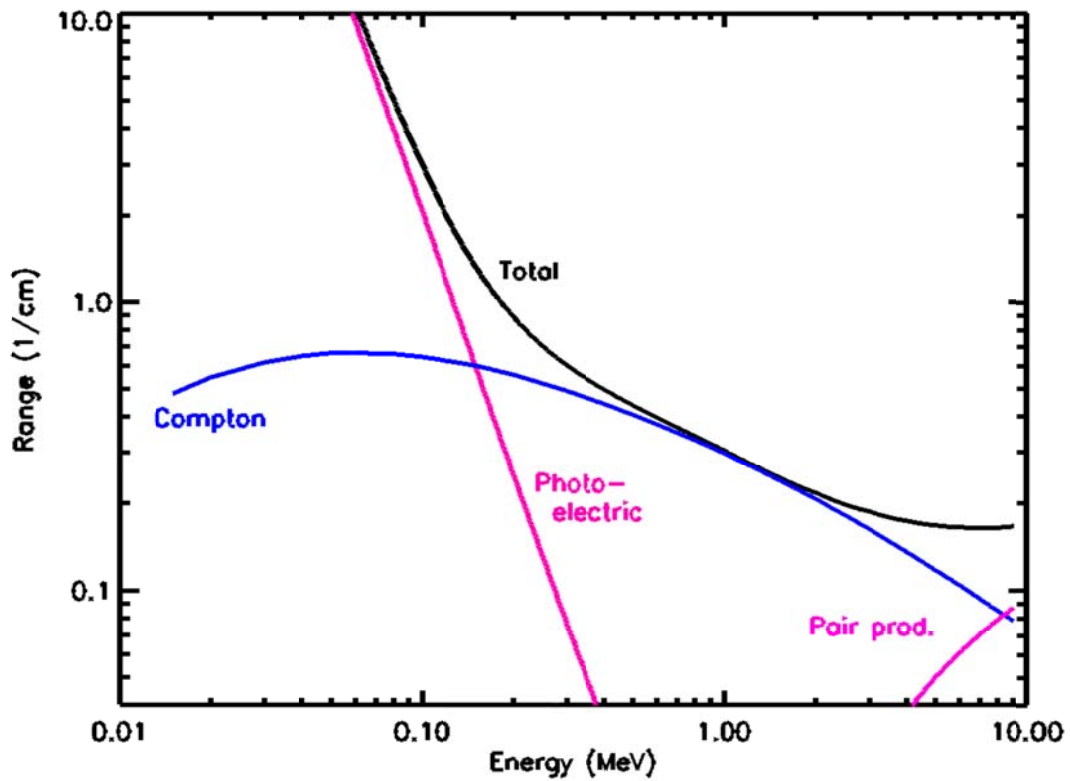
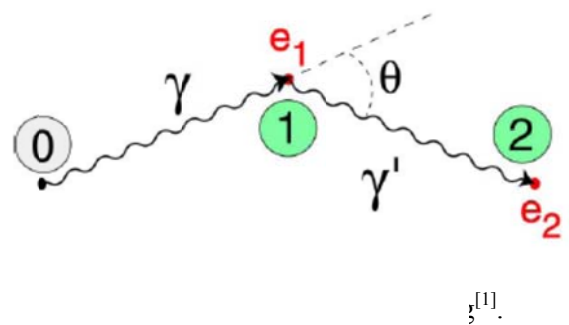


Fig-2: The gamma-ray cross-sections for germanium.

The total attenuation below photon energy of about 100 keV is due nearly entirely to the photoelectric effect. As the photon energy increases above 100 keV, Compton scattering increases until it is the dominant interaction mechanism above few MeV.

### Compton Scattering:

The energy of a  $\gamma$ -ray between a few hundred keV to some MeV is absorbed by Compton Scattering. The energy of the incident  $\gamma$ -ray is partly transferred to the electron to eject it and then the other part of the energy goes into a photon that is scattered. Often several scattering events occur inside the detector with a final photoelectric event. It is the most important event that needs to be considered for tracking a  $\gamma$ -ray. To reconstruct these events we need to determine the scattering angle and the position of the involved interaction with high accuracy.



Let us consider an example as shown in figure-3. A  $\gamma$ -ray scatters with an electron at point 1 and part of its energy ( $e_1$ ) to that electron and again the scattered  $\gamma$ -ray is absorbed at position 2 by the

photoelectric effect. The scattering angle at point 1 is assumed to be  $\theta$ . From the Compton formula, we know that the energy of the scattered photon is given by

$$E_{\gamma'} = \frac{E_{\gamma}}{1 + \frac{E_{\gamma}}{m_0 c^2} (1 - \cos \theta)}$$

Where,  $E_{\gamma'} (= E_{\gamma} - e_1)$ , is the energy of the scattered photon and  $E_{\gamma}$  is the energy of the incident photon and  $e_1$  is the released energy to the Ge Crystal. The energy release at the interaction points and the position of the scattering can be determined by a good position sensitive detector. If we know the source of the  $\gamma$ -ray and 3-D coordinates of the involved points then the scattering angle can be calculated:

$$\cos \theta = \frac{\vec{01} \cdot \vec{12}}{|\vec{01}| |\vec{12}|}$$

Here,  $\vec{01}$  is the vector distance from point 0 to 1 and so is  $\vec{12}$ . From this the energy of the scattered  $\gamma'$ -ray can be determined and the energy can be compared to the energy released at point 2. This procedure can be repeated for a three points system and possibly get alternative values for the Compton scattering. The two energy values can be compared using the energy of the incoming transition with a least-squares:

$$\chi^2 \approx \sum \frac{(E_{\gamma'} - E_{\gamma'}^{\text{expected}})^2}{E_{\gamma'}^{\text{expected}}}$$

Here,  $E_{\gamma'}$  is the observed energy and  $E_{\gamma'}^{\text{expected}}$  is the expected energy of the photon. The  $\chi^2$  is that the photon energy and scattering angle are described by the Compton relationship<sup>[10]</sup>. The sequence of this event is that the  $\gamma$ -ray originates in point **0** has a Compton scattering at point **1** and then the scattered photon is fully absorbed at point **2**. A small value of  $\chi^2$  is expected, for the large value of  $\chi^2$  is against to the model. Sometimes the figure of merit is considered which is inverse of this quantity. We also need to consider other possible scattering sequences like **021** and the least deviation should be accepted as the scattering sequence. It might happen that none of these sequences give a sufficiently small value for  $\chi^2$  because these two interaction points did not exhaust the sum energy as the detector cannot give this information.

If there are N interaction points detected by the detector then there must be N-1 Compton scattering vertices. Then, in general

$$\chi^2 \approx \sum_{n=1}^{N-1} W_n \left( \frac{E_{\gamma'} - E_{\gamma'}^{\text{pos}}}{E_{\gamma}} \right)_n^2$$

Where,  $E_{\gamma}$  and  $E_{\gamma'}$  are the energies of the scattering and scattered  $\gamma$ -rays at the  $n_{\text{th}}$  vertex.  $W_n$  is the weighting factor which is the probability that the  $\gamma$ -rays involves in the  $n_{\text{th}}$  vertex have travelled for the resulting length.

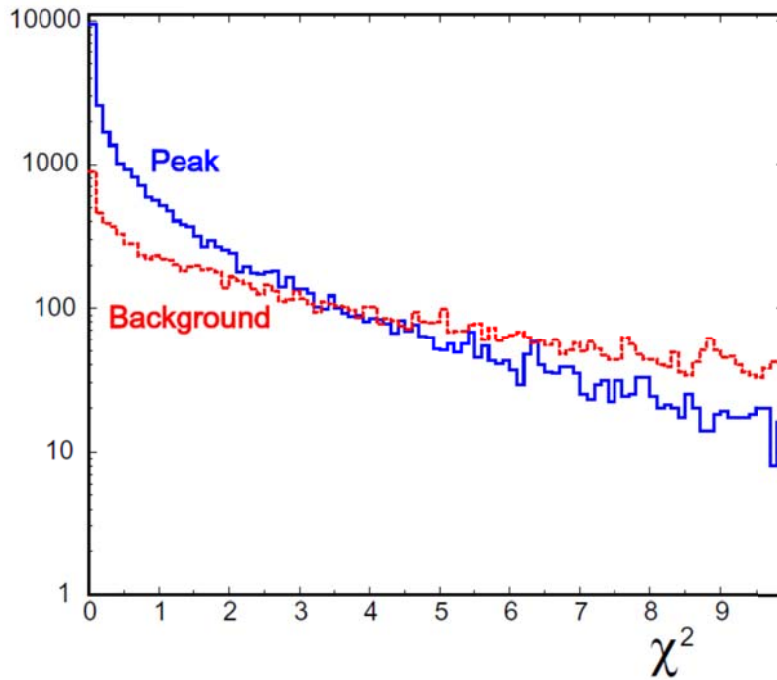


Fig-4: Distribution of  $\chi^2$  for  $10^5$  transitions <sup>[1]</sup>.

There is always some background at any acceptance limit is accepted as shown in figure-4. Here, the distribution of  $\chi^2$  obtained from  $10^5$  transitions with incident  $\gamma$ -ray energy,  $E_\gamma = 1\text{MeV}$  is shown. It is clear that the lower acceptance limits produce better peak-to-total ratio (P/T) ratios. In practice there are always more than one interaction are detected in one event. So, we always have to test the acceptance in two ways: deciding the transition point that belongs to a segment and accept or reject the interaction if it judged to be in background. We could not avoid that the points for different transition are accepted as belonging together as the test is a probabilistic test.

### Pair Production:

Pair production is an important event above a few MeV. Above 9MeV this event overcomes Compton scattering. The minimum energy must be more than the total energy of the  $\gamma$ -ray that collects at the first point of interaction minus  $2m_0c^2$  i.e. the energy needed to create the  $e^-e^+$  pair. Although tracking is complicated in this event this of its mechanism can be easily recognized and reconstructed. The total kinetic energy of the  $e^-e^+$  pair ( $E_\gamma - 2m_0c^2$ ) is shared by the two partners and they are stopped close to the pair production point as both particles are in the MeV range. As they are stopped close to each other the detector usually detects them as one individual energy release. The positron is slowed down and binds to an atomic electron and forms a positronium which annihilates rapidly and emits two collinear 511 keV  $\gamma$ -rays they are escaped or absorbed in some other part of the detector.

### Gamma-Ray Tracking:

Correlating and constructing the multiple interactions of a single  $\gamma$ -ray in a segmented detector is the main technique of  $\gamma$ -ray tracking. The new generation of  $4\pi$  Ge detectors has been developed to significantly improve the efficiency and resolving power of  $\gamma$ -ray spectroscopy. The tracks of the  $\gamma$ -rays in the Ge detector can be constructed in 3D. A detector used for this purpose consists of:

- High-fold segmented Ge detectors
- Digital signal processing electronics
- Pulse-Shape analysis algorithms for real time applications

### High-fold segmented Ge detectors

It is important to know the position of the  $\gamma$ -ray interaction inside the detector with high accuracy (1-2 mm) to get a high efficiency. For this purpose, one Ge detector should consist of 30000 voxels. It is almost impossible to get such a high granularity by a physical segmentation of the crystal. But, the pulse shape analysis method developed for AGATA can provide the position accuracy with high resolution and time information. This method requires only 20-40 segments per detector. The AGATA detectors are Ge-detectors that are 36-fold segment with six-fold azimuthal and six-fold longitudinal segmentation (Figure-5).

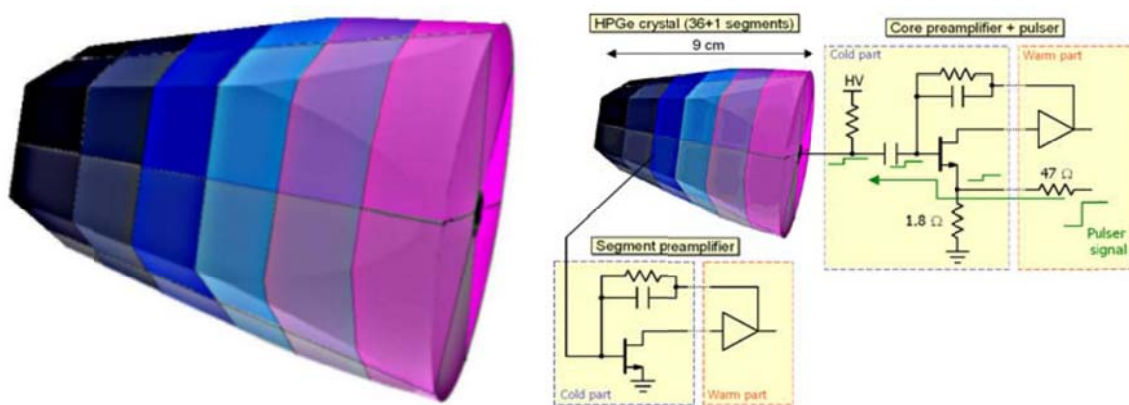


Fig-5: The AGATA 36-fold Ge-detector and individual preamplifiers <sup>[5]</sup>.

The detector is 10 cm long and is circular at the rear side with a diameter of 8 cm and hexagonal at the front face. A common inner electrode and 36 segments are read out via individual preamplifiers. The segments can then be considered as separate detectors.

The parameters for the hexagonal crystals are:

- Maximum cylinder size: 90.0 mm length, 40.00 mm radius
- Coaxial hole size: 10.0 mm diameter, extension to 13.00 mm from the front face
- Passivated areas: 1.0 mm at the back of the detector, 0.6 mm around the coaxial hole.
- Encapsulation: 0.8 mm thickness with a 4.0 mm crystal-can distance
- Cryostat: 1.0 mm thickness with a 2.0 mm capsule-cryostat distance.

By exploiting the spatial information contained in the detector signal we can more accurately localize the  $\gamma$ -ray interaction than is possible by the geometry of the segments. A photoelectron or Compton electron generates electrons and holes which induce image charges of opposite signs on the detector electrodes when a signal is produced. The change of the image charge causes a flow of currents into or out of the electrodes. The induced charge is distributed over several electrodes for the large distance in a multi-segmented detector. For the closer distance an increase and decrease of induced charges of the electrodes continue until the primary charge finally reaches to its destination electrodes and neutralizes the image. To identify the detector sector where the interaction took place we have to observe the net



charge on the charge-collecting electrode simply observing the polarity of the induced signal. This allows for distinguishing between interactions at small and large radii.

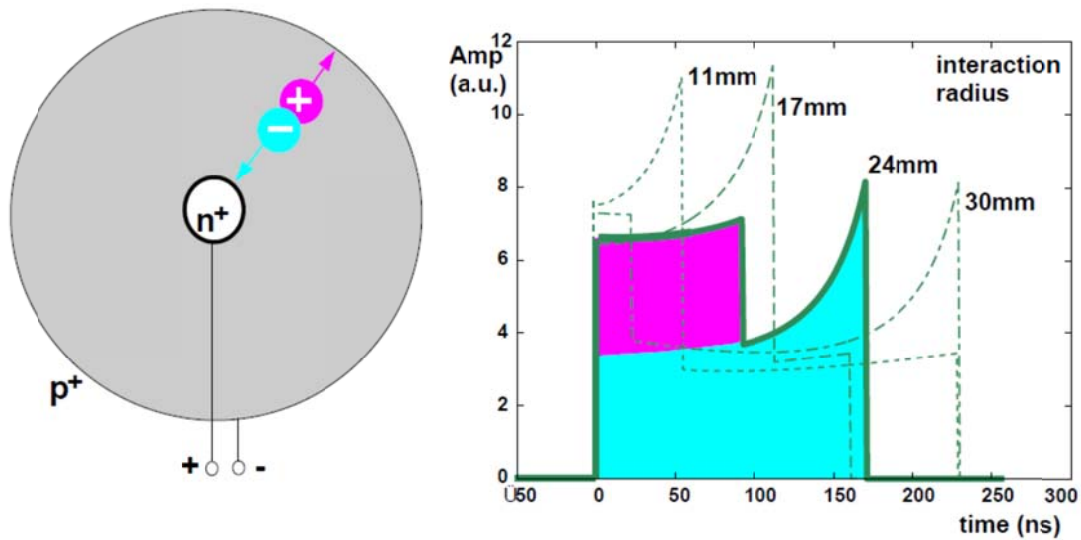


Fig-6: Transversal cut through an n-type coaxial detector (left) with its carrier drift and induced current signals (right) in the detector corresponding to four interaction radii [1].

Carrier drift of an n-type coaxial detector and induced current signals in the detector corresponding to four interaction radii is shown in figure 6. The shapes of the induced current signals are different for different interaction radii. The motion of the charge carriers is determined by the electric field and it depends on the geometry of the detector, the applied voltage and the intrinsic space charge density and charge carrier mobility.

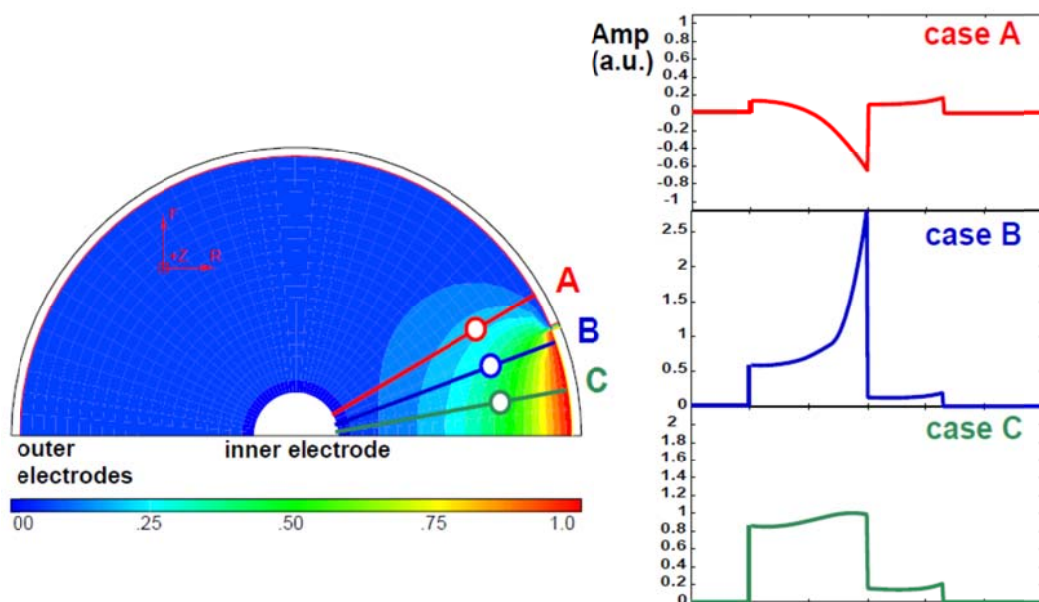


Fig-7: Three different interactions at the same radius with different azimuthal angles in a coaxial detector and the corresponding induced current signals [1].



The weighted potential of a segment in a coaxial detector with three examples of interactions has been shown in the figure 7. The interactions occurring at the same radius but with different azimuthal angles and the corresponding induced current signal are in the right figure. The corresponding mirror (A) and real charge signals (B, C) induced on the segment electrode are shown.

**Digital signal processing electronics:**

The spatial information of the detector signals are known from digital pulse-shape analysis. The pre-amplified detector signal is digitized with 12-bit resolution with a speed of 40 Ms/s. The pre-amplifier signals are digitized with the analog to digital converter (ADC). The  $\gamma$ -ray tracking system required a compact digital signal processing electronics with high computing power. Only five values per interaction is enough for the whole information: energy deposition, its time and three spatial coordinates of the interaction point. Different algorithms have been developed depending on the different detector information.

**Pulse-Shape Analysis:**

The Ge-detector determines the pulse-shape of the  $\gamma$ -ray which contains the information about the three dimensional position of each individual interaction within the detector with the released energy in the interactions. The efficiency of the tracking array depends on these data. We must be able to compare the pulse-shapes to the respective shapes produced by charges each point to extract the position of the interaction. This is done experimentally using tightly collimated  $\gamma$ -ray sources with an external collimated detector for the Compton scattered coincidence. The conductivity of the Ge-detector influences the magnitude of the drift velocities and the angle between the electric field vector and the drift velocity. As a result the shape of the signal is directly influence because the Ge crystal is anisotropic with respect to the crystallographic axis direction. To determine the position of the interaction of the  $\gamma$ -ray one needs to consider the shapes of the induced real and mirror signals. The electrodes of the segment in which an interaction takes place are used to measure the real signals while mirror signals are measured on the neighboring segments where no interaction takes place.

Multi Geometry Simulation [5] is one of the most developed packages for the analysis are uses multi step algorithm. As shown in the figure 8, results from the each stage of the calculation are stored in matrices which are later recalled to generate the pulse shape response which is determined by the charge carriers through the weighted field. The crystal volume is divided into cubic matrices for a given detector. For each position the values of the electrical potential, electric field and weighted field are calculated and the drift velocity matrices are calculated from the electric field matrix.

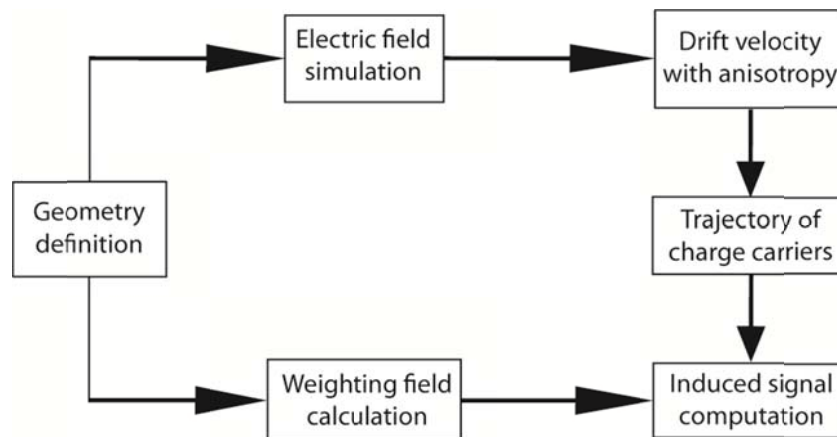


Fig-8: MGS data flow diagram for the simulation of the expected pulse shapes at the contacts of any arbitrary Ge detector geometry <sup>[5]</sup>.

The simulation of the pulse shape for the any arbitrary detector is shown in the figure 8. For a given detector, the crystal volume is divided into a cubic matrix of lattice sites. Values for the electric potential, electric field and weighting field are calculated at each position. The drift velocity matrices are calculated from the electric field matrix. The detector response for a given interaction site is calculated by tracking the trajectory of the charge carriers through the weighting field as shown in figure 8. The steps which should follow to compute the pulse shape response for a given interaction position in the detector volume are:

- Specify the detector geometry.
- Calculate the electric potential surfaces and electric field lines from the solution of the Poisson equation.
- Implement the charge carrier transport in a semiconductor medium.
- Calculate the trajectories of the charge carriers for arbitrary interaction positions.
- Apply Ramo's [11] theorem to recover the charge at the contacts.
- Weight the potential and weight the field resolution.

### Gamma-Ray Path Reconstructing Algorithm:

Reconstructing the path of the  $\gamma$ -ray interaction is one of the main problems of the  $\gamma$ -ray tracking. There are several proposed methods for constructing the path of the  $\gamma$ -ray and two of them are dominating: the back tracking algorithm and clusterisation. The tracking performance is quite sensitive depending on the choice of the formula for the figure-of-merit so; different figures-of-merit have investigated in detail. The influence of the initial momentum of the Compton scattering on the reconstruction results are need to be investigated.

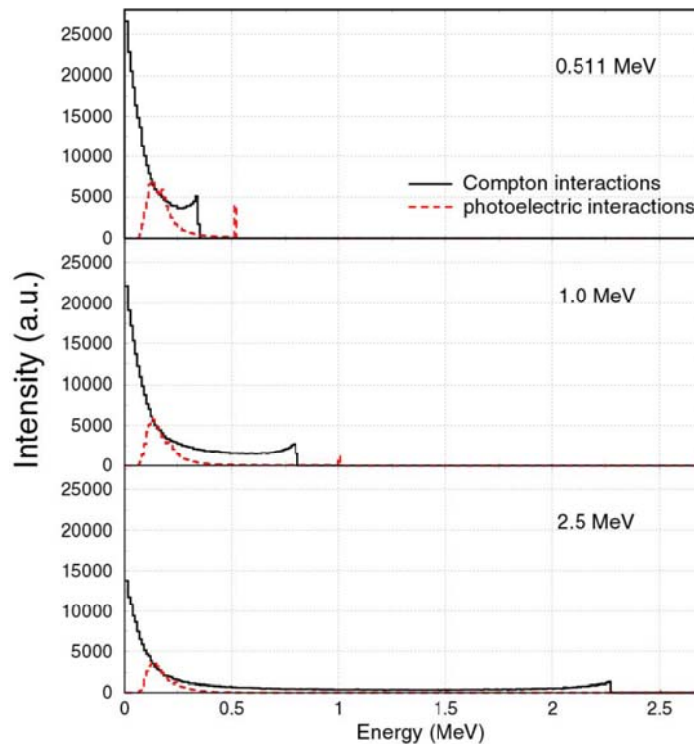


Fig-9: The energy diposition for the photo and Compton spectra <sup>[1]</sup>.

### Backtracking Method:

The backtracking method <sup>[3]</sup> <sup>[4]</sup> of  $\gamma$ -ray reconstruction is based on the observation of the energy deposition of the final photoelectric interaction after scattering. Usually the energy after the interaction falls into a narrow band. In figure 9 the photo and Compton spectra of the energy depositions in the individual interactions of the  $\gamma$ -rays is shown. In most cases the  $\gamma$ -ray interacts by a few Compton scattering events before the photo-absorption takes place. The peak position of the different interactions is distinguishable.

The algorithm starts from the last point of the interaction i.e. the photoelectric interaction whose energy falls in the narrow energy interval. It starts by sorting all the interaction points according to the energy and computes all physical distances between the interaction points. Considering that the first interaction point ( $k=1$ ) has an energy  $E(k)$  greater than  $E_{photomin} = 90$  keV. The nearest interaction point in the Ge detector to the starting point is chosen as the previous interaction point ( $k=2$ ). The compatibility of the distance  $r_{2 \rightarrow 1}$  of these two points is checked with the photoelectric range in Ge for a photon energy  $E_t = E(1)$ :

$$\lambda(E_t) = \frac{1}{\sum (E_t)_{macro}} = \frac{A_{Ge}}{N_{Avogadro} \times \rho_{Ge} \times \sigma(E_t)_{photo}}$$

$\rho_{Ge}$  is the density and  $A_{Ge}$  is the atomic mass of Ge. The probability to travel a distance  $r_{2 \rightarrow 1}$  or more is

$$P(r_{2 \rightarrow 1}) = \exp\left(-r_{2 \rightarrow 1} / \lambda(E_t)\right)$$

The probability is 0 when the distance in Ge is smaller than the physical distance. The probability to undergo a photoelectric effect is

$$P(E_t)_{photo} = \frac{\sigma(E_t)_{photo}}{\sigma(E_t)_{tot}}$$

If the probability  $P(r_{2 \rightarrow 1})$  is smaller than  $P_{photomin}$ , a new photoelectric point is chosen. If the probability  $P(r_{2 \rightarrow 1})$  is greater than  $P_{photomin}$ , the second interaction point ( $k=2$ ) is accepted and the total statistic for this step will be

$$F_{tot,1} = P(r_{2 \rightarrow 1})$$

Before interaction point  $k=2$ , the photon energy was  $E_t = E(1) + E(2)$

After the interaction the scattered energy is  $E_s = E(1)$ . From the Compton formula we know the direction in which the previous point  $k=3$  should search for:

$$\cos(\theta_e) = 1 - m_e c^2 \left( \frac{1}{E_s} - \frac{1}{E_t} \right)$$

Here,  $m_e c^2 = 511$  keV, is the rest mass of the electron.

For the point  $k=3$  we need to look for the distance less than  $3\lambda(E_t)$  away from the  $k=2$  point in the direction of  $\cos(\theta_e)$  which is obtained by testing the difference between  $\cos(\theta_e)$  and  $\cos(\theta_p)$ . Where  $\cos(\theta_p)$  is the geometrical coordinates of the interaction points and given by:

$$\cos(\theta_p) = \frac{\vec{r}_{3 \rightarrow 2} \cdot \vec{r}_{2 \rightarrow 1}}{\|\vec{r}_{3 \rightarrow 2}\| \|\vec{r}_{2 \rightarrow 1}\|}$$

The figure of merit for this difference is

$$F_{\cos} = \exp\left(-\frac{|\cos(\theta_e) - \cos(\theta_p)|}{\sigma_\theta}\right)$$

Where  $\sigma_\theta$  is the uncertainty in the evolution of  $\cos(\theta_p)$  due to the that in the interaction positions. Therefore, the interaction point  $k=3$  is

$$F_{tot,2} = F_{\cos} \times P(r_{3 \rightarrow 2}) \times P(E_t)_{comp}$$

Where,  $P(r_{3 \rightarrow 2})$  is the probability to travel the distance  $r_{3 \rightarrow 2}$  and  $P(E_t)_{comp}$  is the probability to undergo the Compton scattering. If  $F_{tot,2}$  is greater than  $F_{comptmin}$  then this point is accepted. Then the total energy before the interaction point  $k=3$  is:

$$E_t = E(1) + E(2) + E(3)$$

And the scattered energy is:

$$E_s = E(1) + E(2)$$

This procedure is repeated to look for the previous interaction point in the path. When the product of the probabilities at step 3 doesn't satisfy the threshold condition then another interaction point is searched for and so on. If there is no interaction point that fulfills this condition within  $3\lambda$  of the  $k=2$  then the point  $k=3$  is taken to be the source position. Now, we know the source point and as the distance from any interaction point to the source is greater than the average distance between interaction points, so the figure of merit for the angle difference is more severe:

$$F_{\cos} = \exp\left(-2 \frac{|\cos(\theta_e) - \cos(\theta_p)|}{\sigma_\theta}\right)$$

If the source satisfy the threshold requirement and if

$$F_{tot} = \left(\prod_k F_{tot,k}\right)^{(1/k)} > F_{track}, \text{ then the track is ended.}$$

A new choice is made for the interaction point  $k=2$  if the source doesn't fulfill these requirements. These procedures are followed to find all the photoelectric interaction points. If  $E_{photomin} < e$  ( $i$ )  $< E_{photomax}$  is satisfied for no points then the backtracking procedure is complete.

## Mechanical Design for AGATA:

The main construction feature of the AGATA is:

- The detectors are separated by 0.5mm with 15 interchangeable detectors in a radial  $1\pi$  configuration.
- Detectors can be individually removed without touching.
- The array of 15 detectors can rotate from  $-50^\circ$  to  $-110^\circ$  relative to the detector coordinate system.
- The detectors can be moved from 233.8mm to 143.8mm for experiments.
- The detectors can retract to access to the reaction chamber.
- The detector can be modulated to allow for expansion to a  $4\pi$  ball.
- It is movable.

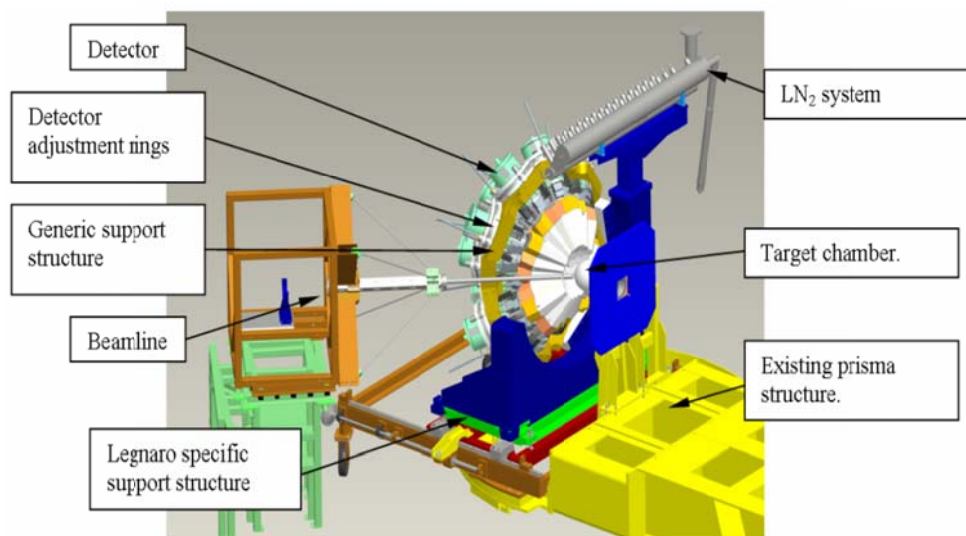


Fig-10:  $1\pi$  detector array <sup>[5]</sup>.

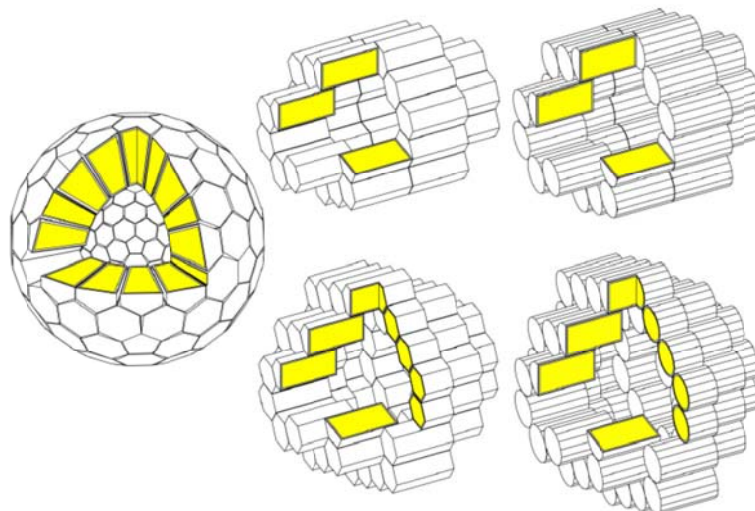


Fig-11:  $4\pi$  arrays built out of regular Ge crystals <sup>[1]</sup>.

Comparison of 120 and 180 hexagon crystal configuration:

No. of Crystal	120	180
Solid angle (%)	72	79
Amount of Ge (kg)	212	320
$\epsilon_{ph}$ / PT at M=1 (%)	38/58	42/58
$\epsilon_{ph}$ / PT at M=30 (%)	20/45	25/48
Inner free space (cm)	16	21*
Number of Clusters/types	40/2	60/1
Rings of clusters	3-7-10-10-7-3	5-10-15-15-10-5
Angular Coverage of Rings	Irregular	Very regular
Electronics channels	4440	6660

### Gamma-Ray Tracking Results:

The algorithm for the  $\gamma$ -ray tracking has been described above. The Monte-Carlo codes have no knowledge of the real detector performance but it contains physical models of the interaction processes. The energy resolution can be taken into account by a random folding of the value provided by the simulation with Gaussian distribution in order to produce a resolution of 2.3 keV FWHM at 1.33 MeV typical for Ge-detectors. The situation is more complicated for the position resolution. Depending on the energy at the interaction point and on the number of interactions per segment and their relative energies the precision is different in different parts of the detector. The points that are closer to each other than the position resolution are packed together to an energy weighted average position.

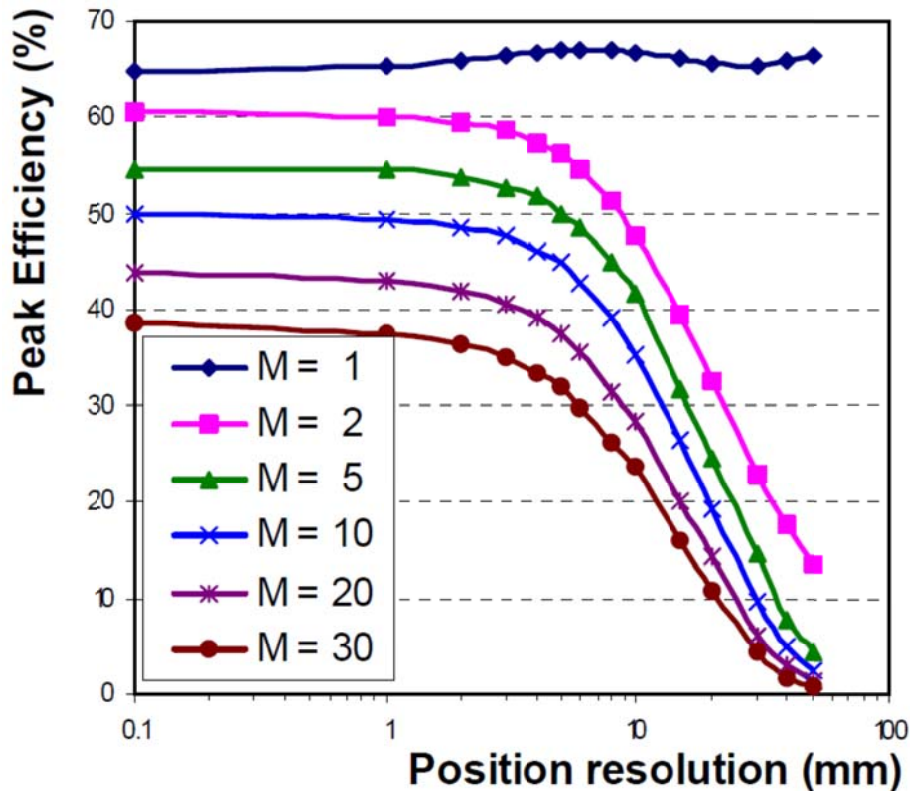


Fig-12: The total peak efficiency as a function of assumed position resolution and  $\gamma$ -ray multiplicity <sup>[1]</sup>.

The figure 12 shows the overall obtained efficiency of a detector as a function of the position resolution for cascades of 1.33 MeV transitions detected in a standard Ge shell. The behavior for the individual transitions is the result of packing points close to each other. The packed points can belong to different transitions as the position resolution becomes an important factor. If the position resolution is worse the losses are bigger and the probability to mix points belonging to different transitions becomes larger at higher multiplicity.

The energy range between 100 keV to 3 MeV for 30 equally spaced transitions of equal intensity for a typical cascade spectrum is shown in the figure 13.

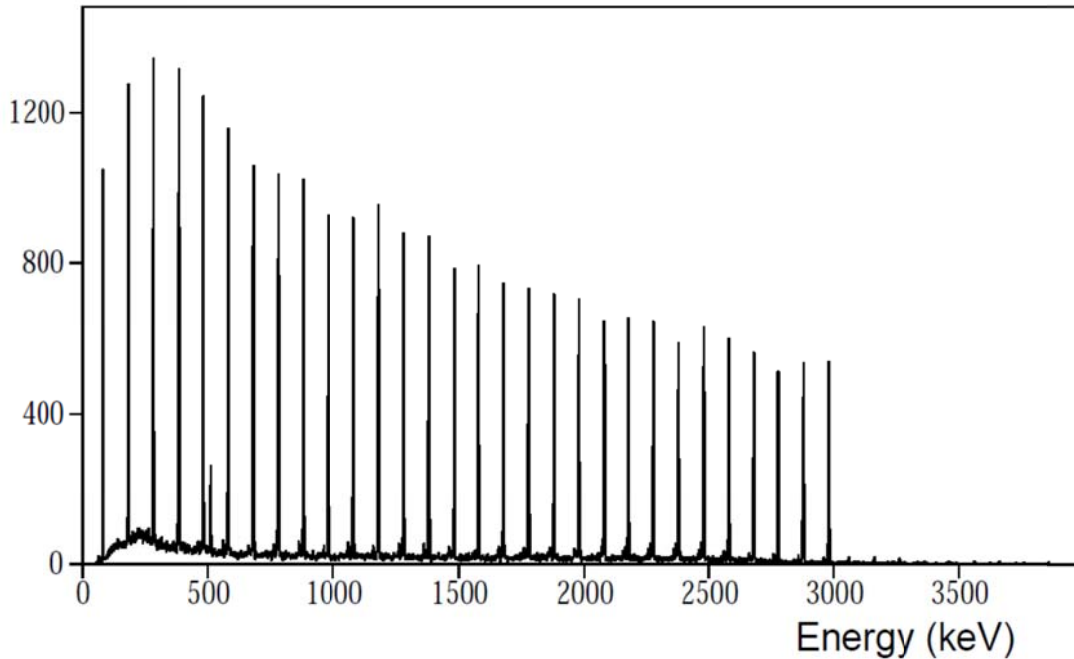


Fig-13: Reconstructed spectrum of a cascade of 30 equally spaced transitions <sup>[1]</sup>.

The background structure shows that some-peaks corresponding to the acceptance of all points of two  $\gamma$ -rays as one transition.

The possibility to obtain precise position information for all  $\gamma$ -ray interactions in the detector array by pulse shape analysis is the principal feature of the AGATA  $\gamma$ -ray tracking. The obtained resolution in this way of the position resolution is much higher than other method. This algorithm can achieve reconstruction efficiency of more than 60% for the position resolution.

In the table below the obtained total peak efficiency and peak to total ratio for AGATA are compared with the performance of the ideal shell and of EUROBALL. The efficiency of the AGATA compared to the EUROBALL is considerable.

Table: Performance of the possible AGATA configurations

Configuration	No. of detectors (Crystals)	Amount of Ge (kg)	$\epsilon_{ph}$ [P/T]% $M_\gamma=1$	$\epsilon_{ph}$ [P/T]% $M_\gamma=30$
Ideal $4\pi$ shell	1	233	65 [85]	36 [60]
AGATA 120	40 (120)	212	33 [54]	19 [44]
AGATA 180	60 (180)	320	38 [53]	24 [44]
EUROBALL	71 (239)	210	9 [56]	6 [37]



## Summary:

AGATA is the most efficient  $\gamma$ -ray tracking array ever developed and position sensitive Ge-detectors are the main concept for this. It is mentionable that the *Composite Ge detectors* were first developed for the EUROGAM spectrometer and it has been used many standard applications. The *Encapsulated Ge detectors* were developed for the EUROBALL spectrometer. The *Segmented techniques* are the latest of their combination and are used in AGATA. In this paper, a short overview of the AGATA is given.

## References:

- [1] Ed. Gerl J and Korten W, AGATA Technical Proposal (2001).
- [2] J Simpson, J. Phys. G: Nucl. Part. Phys. 31 S1801-S1806 (2005).
- [3] L. Milechina and B. Cederwall, Nuclear Instruments and Methods in Physics Research Section A 508, Issue 3, 394-403 (2003).
- [4] A. Lopez-Martens, K. Hauschild, A. Korichi, J. Roccaz and J-P. Thibaud, Nuclear Instruments and Methods in Physics Research Section A 533, Issue 3, 454-466 (2004).
- [5] Ed. J. Simpson, J. Nyberg, W. Korten, AGATA Technical Design Report (2008).
- [6] <http://www-win.gsi.de/agata/>
- [7] Dino Bazzacco, Nuclear Physics A 746, 248-254 (2004).
- [8] J. Gerl, Nuclear Physics A 752, 688-695 (2005).
- [9] Th. Kroll and D. Bazzacco, Nuclear Instruments and Methods in Physics Research, A 565, Issue 2, 691-703 (2006).
- [10] L. Anderson, Compton Scattering, (Nov. 2007).
- [11] S. Ramo Proc. I.R.E. 27, 584 (1939).
- [12] Ed. D. Balabanski, D. Bucurescu, AGATA Physics case, Internal Report (2008).
- [13] Joa Ljungvall and Johan Nyberg, Nuclear Instruments and Methods in Physics Research, A 550, Issues 1-2, 379-391 (2005)